**JOURNAL OF THEORETICAL
AND APPLIED MECHANICS**
62, 3, pp. 477-490, Warsaw 2024
https://doi.org/10.15632/jtam-pl/189316

STUDY ON A CONCISE AND UNIFIED UNSTABLE CREEP MODEL FOR ROCKS

Yang Cheng
College of Architectural Engineering, Tongling University, Tongling, China
e-mail: chengytl@163.com

Liangliang Zhang
School of Civil Engineering and Architecture, Anhui University of Science and Technology, Huainan, China
e-mail: zllaust@163.com

The unsteady creep curve of rocks is antisymmetric to the dynamic surface subsidence curve of coal mining. Accordingly, a four-parameter unsteady creep model of rock was established using an analogous reasoning method from the perspective of phenomenology, and a simple method for determining the model parameters was proposed. The test curves of four different types of rocks were in good agreement with the theoretical curves of the model. In particular, the accelerated creep test curves with nonlinear characteristics were consistent with the theoretical curves of the model, verifying the rationality and accuracy of the model.

Keywords: rock mechanics, creep model, antisymmetric, unsteady creep, damage

1. Introduction

The creep behavior of rocks is a key factor affecting the safety and long-term stability of a structure (Wei *et al.*, 2019). When the external load is less than the long-term strength of the rock, the creep that occurs in the rock is steady, which includes instantaneous strain, attenuation, and constant velocity creep stages. This type of creep can be described using classic creep models (the Burgers, Bingham, and Nishihara models) (Song *et al.*, 2023). Theoretical and practical engineering applications of these creep models have been well established. When the external load is greater than the long-term strength of the rock, unsteady creep occurs in the rock, which includes instantaneous strain, attenuation creep, constant-velocity creep, and accelerated creep stages (Jin *et al.*, 2024). The establishment of an unsteady creep model for rock is an important and difficult task in rock mechanics (Taheri *et al.*, 2020).

Existing creep models can be divided into the following categories: empirical creep model (Zhang *et al.*, 2013; Zivaljevic and Tomanovic, 2022), component combination creep model (Zhao *et al.*, 2019; Zhang *et al.*, 2011) and improved component combination creep model based on nonlinear rheology theory (Zhang and Wang, 2020; Yang *et al.*, 2014), creep damage theory (Yang *et al.*, 2015; Song and Li, 2022) and fractional order theory (Zhou *et al.*, 2011; Liu *et al.*, 2021). Empirical creep models establish mathematical expressions for strain and time through curve fitting based on existing creep test data. The creep equations of such models are simple in form, with high precision and few parameters. However, owing to the unclear physical meaning of parameters and the short creep test time compared with the actual creep process of rock mass, the creep characteristics of the rock reflected by this model are quite different from the actual rock mass; therefore, it is only suitable for describing the creep process of specific rocks under specific test conditions. However, it has rarely been applied to the study of creep characteristics in rock engineering. The component-combination creep model combines elastic, plastic, and viscous components through different forms of series and parallel connections to obtain a combination model that can describe rock elasticity, viscosity, viscoelasticity, and viscoplasticity. The physical meaning of these model parameters is clear, and the creep equation can be derived easily. The component-combination creep model is more widely applicable than the empirical creep model because of its variable combination forms. However, because the model parameters of this type of creep model are constant, this model can only describe the steady creep of rock and cannot describe unsteady creep. Therefore, this model is not suitable for analyzing the actual creep failure in rock mass engineering (Discenza *et al.*, 2020).

The improved component-combination creep model reflects nonlinear characteristics of the accelerated creep process of rocks by concatenating nonlinear damage bodies based on the component-combination model or by replacing the nonlinear creep model parameters with the component-combination creep model parameters, thereby establishing a mechanical model that can describe the unsteady creep process of rocks. Compared with the empirical creep model and component combination creep model, this type of model has been greatly improved in theory and practice; however, it still has the following two shortcomings. (1) The creep equation is too complicated. In the process of constructing the unsteady rock creep model, four different equations are often used to describe the instantaneous strain stage, attenuated creep stage, constant velocity creep stage, and accelerated creep stage in segments (such as using elastic elements to describe the instantaneous strain, Kelvin bodies to describe the attenuated creep stage, viscous bodies to describe the constant-velocity creep stage, and time-dependent deteriorated viscoplastic bodies to describe the accelerated creep stage). Then, according to the superposition principle, these four equations are superimposed to establish a mechanical model that can describe the unsteady creep process of rocks. Although the physical meaning and function of each part of the improved creep model established by this method are clear, and the constitutive and creep equations are easy to deduce, the form of the final creep equation is too long and complicated because of the large number of functions, which is not conducive to numerical simulation analysis and practical engineering applications. In addition, the four equations are independent of each other and there is no unified equation to describe the unsteady creep process in rocks. (2) The creep model has several parameters. The improved creep model improves the accuracy of the model by introducing undetermined parameters, but at the same time, introducing new model parameters increases the difficulty of parameter determination. Moreover, owing to the complexity of the improved creep model, the creep equation contains many undetermined parameters, usually more than 7 (Yan *et al.*, 2020). Such many creep parameters are difficult to determine accurately based on limited test data. Therefore, although the improved component combination creep model can describe the unsteady creep process of an indoor rock test well, owing to the limitation of the number of parameters, it is difficult to effectively analyze the creep mechanical properties of actual engineering rock masses.

In summary, to facilitate finite element software programming and actual creep failure process analysis of rock mass, it is urgent to establish a mechanical model of rock creep with fewer parameters and a unified creep function, which should be able to describe instantaneous strain, attenuated creep, constant velocity creep, and accelerated creep characteristics of rock simultaneously. In view of this, this study establishes a rock unsteady creep model with four model parameters only by an analogy reasoning method from the perspective of phenomenology, and provides a method to determine the model parameters, which provides a reference for the study of rock creep characteristics.

2. Four-parameter unsteady creep model

Many on-site monitoring data and theoretical studies have shown that the subsidence process of a certain point of the surface caused by coal mining is composed of three parts: the initial subsidence stage, the rapid subsidence stage and the decay subsidence stage, and it is approximately an "S" shaped curve with time, as shown in the red curve in Fig. 1. While the typical unsteady creep curve of rock is approximately an inverse "S" curve, as shown by the blue curve in Fig. 1. Therefore, the dynamic surface subsidence curve exhibits an antisymmetric relationship with the unsteady creep curve. Therefore, the surface dynamic subsidence function is first determined, and then the inverse function of the surface dynamic subsidence function is obtained by considering $\varepsilon(t) = t$ as the symmetry axis, which can yield a unified functional form describing the unsteady creep process of rocks. According to the basic mathematical theory, the functions represented by the red and blue curves are inverse functions of each other. Therefore, if the surface dynamic subsidence function is determined and its inverse function is obtained, the unsteady creep function of the rock can be established.

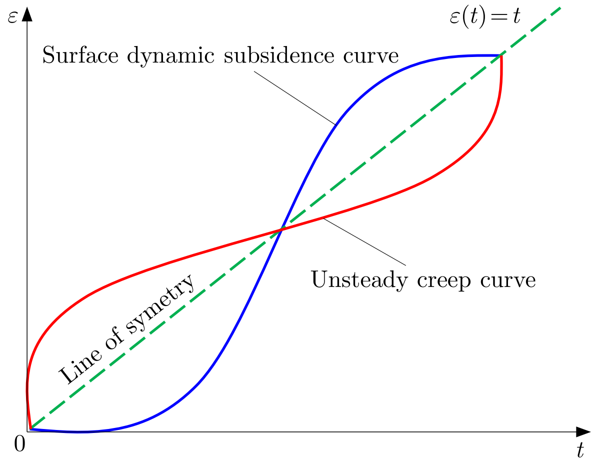

Fig. 1. Demonstration of the unsteady creep curve

The analysis indicates that the key to establishing a mechanical model that can reflect the unsteady creep process of rocks is to determine an "S" type function that can describe the surface dynamic subsidence law with time. Based on the classic Knothe time model (Hejmanowski, 2015), an improved Knothe time model was established by proposing new model assumptions (Zhang *et al.*, 2020) that could accurately describe the surface dynamic subsidence process caused by coal mining. The model function is expressed as follows

$$W(t) = W_0[1 - \exp(-Ct^n)] \tag{2.1}$$

where $W(t)$ is the surface dynamic subsidence, W_0 is the final surface subsidence, C is the time influence coefficient related to the mechanical properties of the overlying strata, t is time, and n is the model order.

The surface dynamic subsidence curves for different model orders n are shown in Fig. 2.

From Fig. 2, under different n conditions, the surface dynamic subsidence curves are all of "S" type, which is antisymmetric with the unsteady creep curves of rocks. Therefore, the unsteady creep models of rocks can be established by determining the inverse function of (2.1).

In Eq. (2.1), time t is the independent variable and $W(t)$ is the dependent variable; its inverse function expression is obtained as follows

$$t = \Big[-\frac{1}{C}\ln\Big(1 - \frac{W(t)}{W_0}\Big)\Big]^{\frac{1}{n}} \tag{2.2}$$

In Eq. (2.2), $W(t)$ is the independent variable and time t is the dependent variable. In the creep function, the independent variable is time t and the dependent variable is strain ε. Therefore, the function expression of the unsteady creep model of the rock can be obtained by analogous reasoning as follows

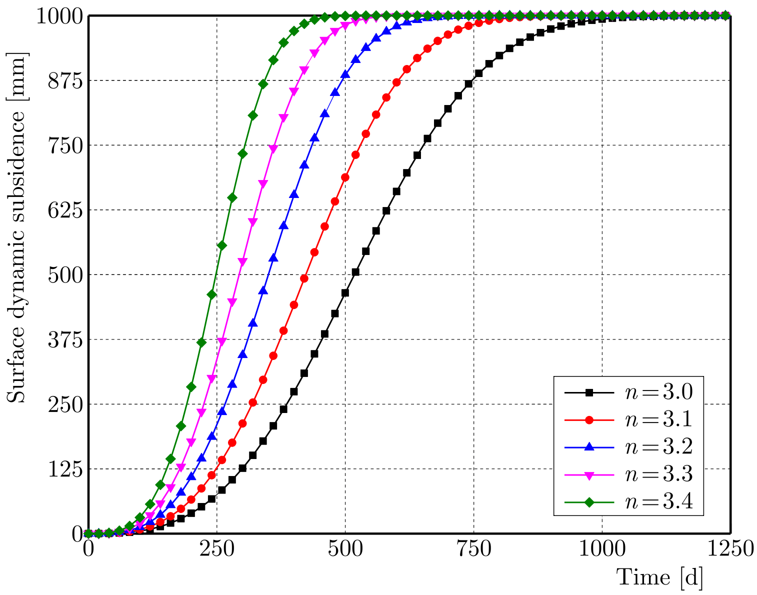

Fig. 2. Surface dynamic subsidence curves

$$\varepsilon = \Big[-\frac{1}{C}\ln\Big(1-\frac{t}{W_0}\Big)\Big]^{\frac{1}{n}} \tag{2.3}$$

In Eq. (2.1), W_0 is the final surface subsidence, which is the maximum value of the independent variable $W(t)$, then W_0 in Eq. (2.3), and is the maximum value at time t, that is, the time when the rock undergoes creep failure. Parameter C in Eq. (2.1) is the time influence coefficient related to mechanical properties of the overlying strata. This parameter is related to the physical and mechanical properties of the strata and time, and is expressed as viscosity in the rock creep model. Simultaneously, because the creep characteristics of the rock are closely related to the stress level σ, $\sigma/\eta = 1/C$ can be set, and Eq. (2.3) can be further expressed as

$$\varepsilon = \Big[-\frac{\sigma}{\eta}\ln\Big(1-\frac{t}{t_f}\Big)\Big]^{\frac{1}{n}} \tag{2.4}$$

where η is the viscosity coefficient of the rock and t_f is the time when the rock undergoes creep failure.

The creep model function established by Eq. (2.4) represents the variation in the creep strain with time and does not include the instantaneous strain stage in the unsteady creep process of rocks. Therefore, to reflect the entire creep process, it is necessary to add an instantaneous strain that is only related to the stress level but independent of time based on Eq. (2.4), which can be represented by an elastic element. Based on the above analysis, a four-parameter unsteady creep mechanics model is established, as shown in Fig. 3.

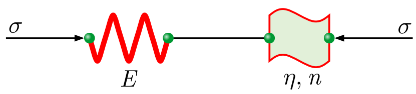

Fig. 3. Four-parameter unsteady rock creep model

According to the stress-strain relationship of the series and parallel connections, the unsteady creep equation of the rock is obtained as follows

$$\varepsilon = \frac{\sigma}{E} + \Big[-\frac{\sigma}{\eta}\ln\Big(1-\frac{t}{t_f}\Big)\Big]^{\frac{1}{n}} \tag{2.5}$$

where E is the elastic modulus of the elastic element.

We derived Eq. (2.5) and obtained the creep velocity and acceleration as follows

$$
\begin{aligned}
\varepsilon' &= \frac{1}{n}\frac{\sigma}{\eta}\frac{1}{t_f - t}\Big[-\frac{\sigma}{\eta}\ln\Big(1-\frac{t}{t_f}\Big)\Big]^{\frac{1-n}{n}} \\
\varepsilon'' &= \frac{1}{(t_f - t)^2}\Big\{\Big(\frac{\sigma}{\eta}\Big)^2\frac{1}{n}\Big[\frac{1-n}{n} - \ln\Big(1-\frac{t}{t_f}\Big)\Big]\Big[-\frac{\sigma}{\eta}\ln\Big(1-\frac{t}{t_f}\Big)\Big]^{\frac{1-2n}{n}}\Big\}
\end{aligned}
\tag{2.6}
$$

According to Eq. (2.6), the creep rate is always greater than zero, indicating that the creep strain gradually increases with time, which is consistent with the actual situation. The critical moment for rock creep acceleration to be 0 is $\{1 - \exp[(1/n) - 1]\}t_f$, and when the creep time does not reach this critical value, the creep acceleration is always less than 0, indicating that the rock creep rate gradually decreases during this stage. When the creep time is between this critical value and the time when the rock undergoes creep failure, the creep acceleration is always greater than 0, indicating that the rock rate gradually increases with time at this stage. Therefore, the moment when the creep acceleration is 0 is not only the moment when the rock creep rate is minimum, but also the starting point of the accelerated creep stage. The above analysis indicates that the four parameter rock non-stationary creep model cannot strictly meet the creep deformation laws of the entire rock process, especially the creep rate characteristics during the constant velocity creep process. However, the constant velocity creep does not mean that the creep rate remains strictly unchanged, but the amplitude of change is relatively small (Wang *et al.*, 2018). Therefore, the four parameter rock unsteady creep model is reasonable and feasible for reflecting the complete creep process of rocks.

3. Model parameters determination

From Eq. (2.5), the creep equation contains only four model parameters E, η, t_f, n, which greatly reduces the number of parameters compared to other complex creep models and is beneficial for practical engineering applications. The creep curves of the rocks at different stress levels are shown in Fig. 4. At low stress levels, there was no accelerated creep stage in the creep curve; however, an accelerated creep process occurred at medium and high stress levels. Moreover, the creep failure time at a high stress was significantly shorter than that at a medium stress. Based on the characteristics of rock creep curves under different stress states, as shown in Fig. 4, a simple and feasible method for determining creep model parameters was proposed.

Determination of elastic modulus E

The instantaneous elastic strain ε_e is generated during rock loading and can be described by an elastic element. Based on the elastic constitutive relationship, the elastic modulus E is determined as

$$
E = \frac{\sigma}{\varepsilon_e} \tag{3.1}
$$

Determination of t_f

Without considering the influence of the rock occurrence environment, the creep failure time of rocks is only a function of stress; therefore, $t_f = f(\sigma)$. As shown in Fig. 4, the creep failure time decreases with an increase in the stress level. According to the Kachanov material creep damage rate theory (Kachanov, 1992), the time at which the rock undergoes creep failure can be determined using the following equation

$$
\frac{dD}{dt} = k\Big(\frac{\sigma}{1-D}\Big)^{v} \tag{3.2}
$$

where dD/dt is the damage rate, D is the damage variable, k, v are rock material constants.

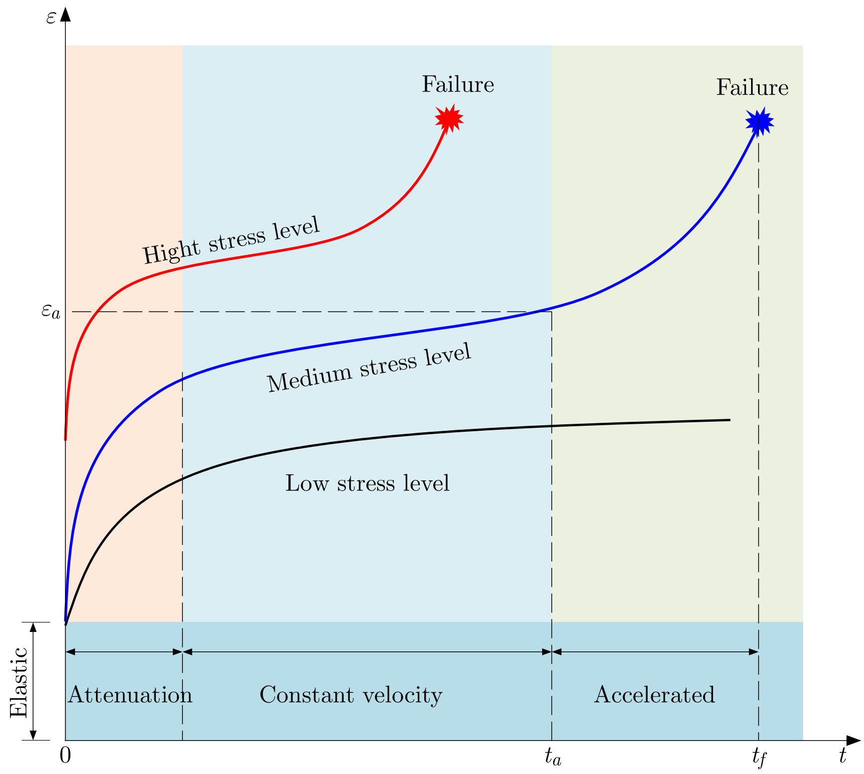

Fig. 4. Creep curves of rocks under different stress levels

Assuming that the damage variable is equal to one when the rock undergoes creep failure, the expression for the rock failure time obtained from Eq. (3.2) is

$$t_f = \frac{1}{C(1+\upsilon)\sigma^{\upsilon}} \tag{3.3}$$

Through the unsteady creep test curve of rock under different stress levels, the material constants k, υ can be determined, and then the functional relationship between rock creep failure time and stress level can be obtained.

Determination of η, n

The corresponding time for the rock to enter the accelerated creep stage from the constant--velocity creep stage in Fig. 4 is t_a, and the corresponding strain is ε_a. Because the creep acceleration of rock is zero when the creep velocity reaches its minimum value

$$t_a = \Big[1 - \exp\Big(\frac{1}{n} - 1\Big)\Big] t_f \tag{3.4}$$

The expression for n obtained from Equation (3.4) is

$$n = \Big[1 + \ln\Big(1 - \frac{t_a}{t_f}\Big)\Big]^{-1} \tag{3.5}$$

When $t = t_a$, $\varepsilon = \varepsilon_a$ according to Eq. (2.4), there is

$$\varepsilon_a = \frac{\sigma}{E} + \Big[-\frac{\sigma}{\eta}\ln\Big(1 - \frac{t_a}{t_f}\Big)\Big]^{\frac{1}{n}} \tag{3.6}$$

The expression for η obtained from Eq. (3.6) is

$$\eta = -(\varepsilon_a - \varepsilon_e)^{-n}\sigma \ln\Big(1 - \frac{t_a}{t_f}\Big) \tag{3.7}$$

In summary, all four parameters of the unsteady creep model of the rock were determined. Meanwhile, the creep model parameters can also be obtained through curve fitting based on rock creep experimental data.

4. Model validation

The rationality and accuracy of the four-parameter rock unsteady creep model established in this study were verified by referring to the uniaxial compression creep test results for four different types of rock. The creep model parameters of the four types of rock under different stress levels were obtained by curve fitting of experimental data. A comparison between the theoretical curve of the four-parameter rock unsteady creep model and the test results is shown in Figs. 5-8.

Table 1. Model parameters of different types of rocks

Rock	σ [MPa]	E [GPa]	t_a [h]	ε_a [10^{-3}]	n	η [GPa h]	t_f [h]	C	υ
Schist (Sterpi and Gioda, 2009)	34.30	7.49	169.2	5.38	3.22	$1.67 \cdot 10^{-6}$	338.4	$6.12 \cdot 10^{-9}$	3.29
	39.40	7.91	98.5	5.72	2.60	$2.59 \cdot 10^{-4}$	214.3		
Changshan salt rock (Cao *et al.*, 2020)	14.41	40.14	538.0	0.49	4.36	$7.21 \cdot 10^{-11}$	1030	$9.56 \cdot 10^{-57}$	44.32
	14.72	33.38	215.5	0.58	3.83	$1.26 \cdot 10^{-13}$	401		
Qiaohou salt rock (Zhong & Ma, 1987)	7.77	2.69	114.8	1.18	2.20	0.76	273	$1.71 \cdot 10^{-3}$	0.26
	11.3	1.71	86.4	1.70	1.75	0.14	248		
Sandy shale rock (Zhong & Ma, 1987)	52.82	28.40	8.5	2.27	5.42	$1.23 \cdot 10^{-14}$	15.30	$1.69 \cdot 10^{-25}$	15.30
	55.37	28.69	4.6	2.32	5.11	$1.21 \cdot 10^{-13}$	8.34		
	56.64	27.23	3.2	2.37	4.37	$1.46 \cdot 10^{-11}$	5.96		
	58.31	27.50	1.9	2.45	4.32	$9.7 \cdot 10^{-12}$	3.56		

As can be seen from the comparison results in Figs. 5-8, the four-parameter rock unsteady creep model can not only describe the instantaneous strain stage, attenuation creep stage, and constant velocity creep stage of different types of rocks under different stress levels but also reflects the accelerated creep stage with particularly obvious nonlinear characteristics, and its rationality has been verified. The theoretical curve of the model is in good agreement with the test results, indicating that the model can accurately predict the creep strain trends of different types of rocks under different stress levels over time, effectively design support forms, and determine the support construction time. In addition, Eq. (2.4) shows that the model can describe the unsteady creep process of rocks in a simple and unified expression, overcoming the shortcomings of complex creep equations and numerous model parameters in component combination models, which are more conducive to engineering applications.

To further verify the accuracy of the four-parameter rock unsteady creep model, the relative standard deviation between the test and theoretical creep values for the four types of rocks was calculated without considering the error of the test data. The calculation formula is shown in Eq. (4.1) (Zhao *et al.*, 2020). The calculation results show that the relative standard deviations between the test and theoretical values of schist under stress levels of 34.3 MPa and 39.4 MPa are 0.83% and 0.55%, respectively, which are basically negligible. The relative standard deviations between the test values and theoretical values of Changshan salt rock under stress levels of 14.41 MPa and 14.72 MPa are 2.87% and 1.55%, respectively. The relative standard deviations

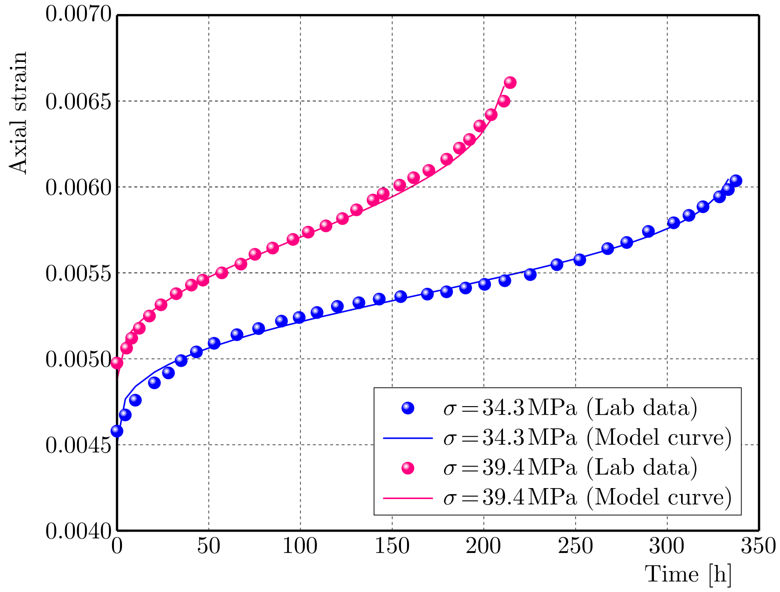

Fig. 5. Comparison between test and theoretical curves for schist

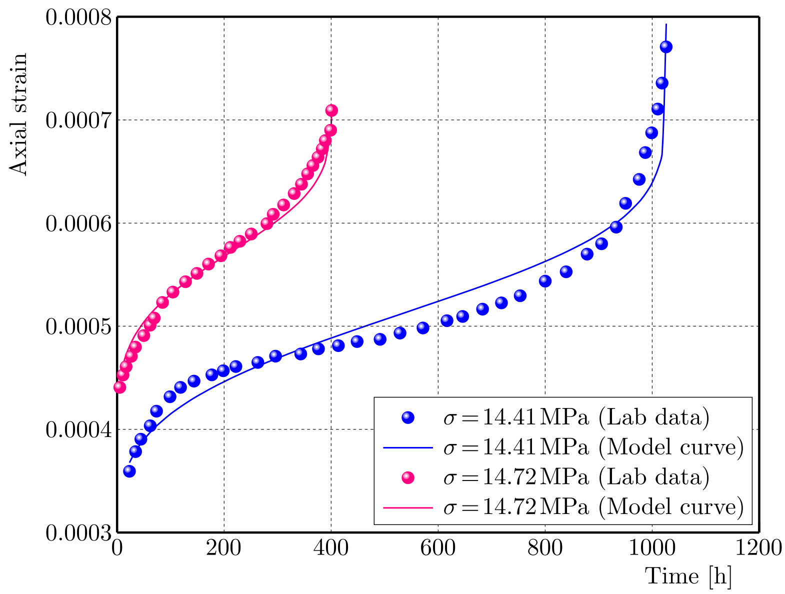

Fig. 6. Comparison between the test and theoretical curves for the Changshan salt rock

between the test values and model theoretical values of Qiaohou salt rock under stress levels of 14.41 MPa and 14.72 MPa are 4.83% and 4.94%, respectively. The error of Qiaohou salt rock is slightly larger than that of Changshan salt rock, but it is still within the allowable range. The relative standard deviations between the test and theoretical values of sandy shale at stress levels of 52.82, 55.37, 56.64 and 58.31 MPa are 1.15%, 1.05%, 0.80%, and 0.82%, respectively. The relative standard deviations of sandy shale at the four stress levels were small. The above calculations indicate that the relative standard deviation between the creep test values and the theoretical values of the four types of rocks was less than 5%. Error analysis further confirmed the accuracy of the four-parameter rock unsteady creep model

$$m = \sqrt{\frac{1}{N-1}\sum_{i=1}^{N}(\varepsilon_s - \varepsilon_l)^2} \qquad f = \frac{m}{\varepsilon_f} \tag{4.1}$$

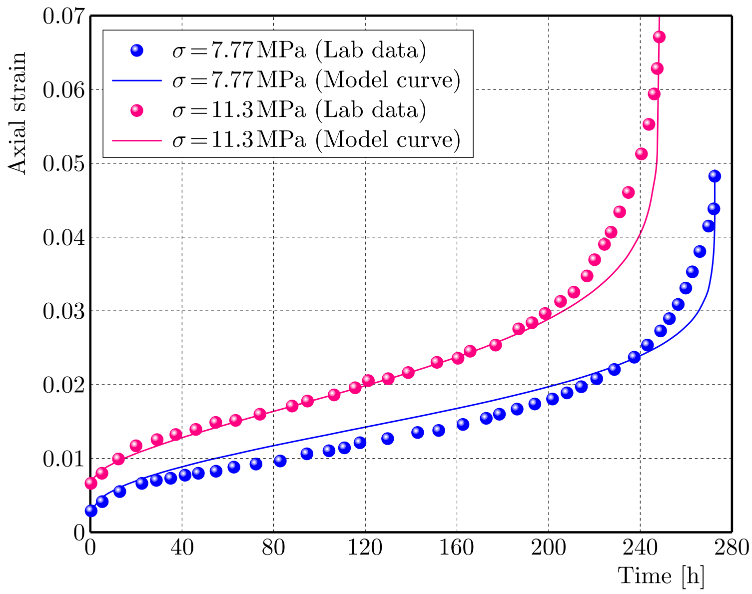

Fig. 7. Comparison between test and theoretical curves for Qiaohou salt rock

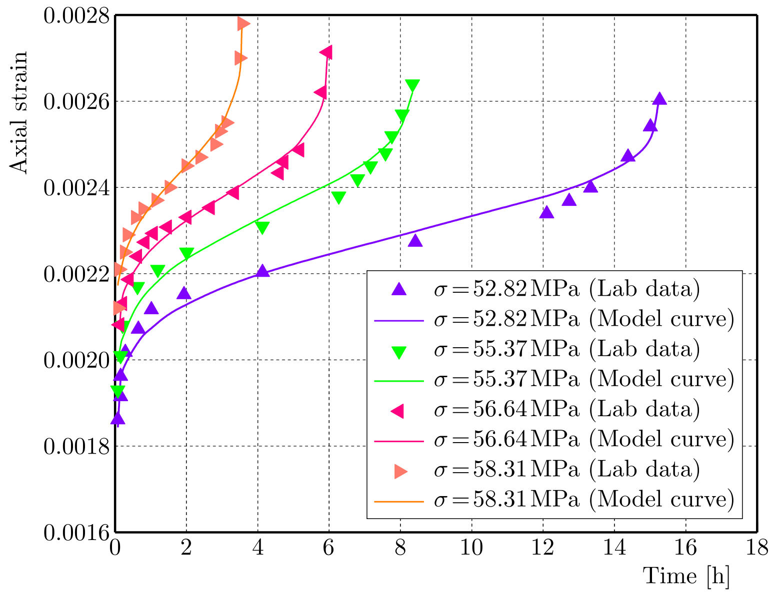

Fig. 8. Comparison between the test and theoretical curves for sandy shale rock

where m is the standard deviation, f is the relative standard deviation, and are the test and theoretical values. ε_f is the strain on the rock during the creep failure. N is the number of samples.

5. Model parameter analysis

The rock unstable creep model established in this paper only contains four model parameters, which has the advantage of few parameters and high accuracy. This Section discusses the local influence of the four model parameters on the rock unstable creep curve.

5.1. The influence of E

Assuming $\sigma = 60\,\mathrm{MPa}$, $\eta = 2.0 \cdot 10^{-12}\,\mathrm{GPa\,h}$, $t_f = 15\,\mathrm{h}$, $n = 4$, according to Eq, (2.5), the unsteady creep curves of the rocks corresponding to different elastic modulus E were obtained, as shown in Fig. 9.

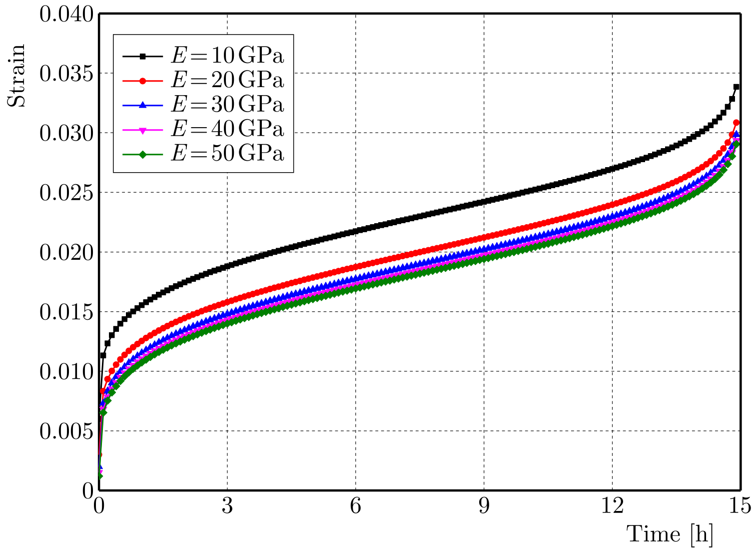

Fig. 9. Influence of E on the creep curve

Figure 9 shows that a change in E does not affect the shape of the model creep curve and creep strain, but only affects the instantaneous elastic strain. With an increase in E, the instantaneous strain at the same time gradually decreases. In addition, Fig. 9 shows that, under the same E value increment, the reduction in instantaneous strain gradually decreases; that is, according to the order from bottom to top, the model creep curve becomes increasingly sparse from dense. This indicates that when the value of E is small, a change in its value significantly influences the instantaneous elastic strain of the model. However, when the value of E was large, a change in its value had little influence on the instantaneous elastic strain.

5.2. The influence of η

Assuming $\sigma = 60\,\mathrm{MPa}$, $E = 30\,\mathrm{GPa}$, $t_f = 15\,\mathrm{h}$, $n = 4$, according to Eq. (2.5), the unsteady creep curves of the rocks corresponding to different viscosity coefficients η were obtained, as shown in Fig. 10.

Figure 10 shows that a change in η has little effect on the shape of the model creep curve; however, with an increase in η, the creep stress variable at the same time gradually increases. In addition, Fig. 10 shows that, under the same η value increment, the creep strain increment simultaneously gradually decreases; that is, according to the order from bottom to top, the model creep curve becomes increasingly dense from sparse. This indicates that when the value of η is small, a change in its value significantly influences the creep strain of the model. However, when the value of η was large, the change in its value had little influence on the creep strain.

5.3. The influence of t_f

Assuming $\sigma = 60\,\mathrm{MPa}$, $E = 30\,\mathrm{GPa}$, $\eta = 2.0 \cdot 10^{-12}\,\mathrm{GPa\,h}$, $n = 4$, according to Eq. (2.5), the unsteady creep curves of the rocks corresponding to different t_f were obtained, as shown in Fig. 11.

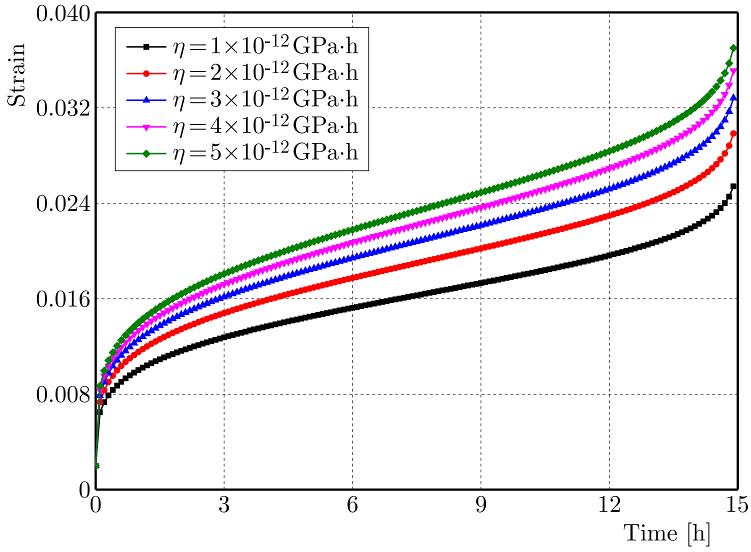

Fig. 10. Influence of η on the creep curve

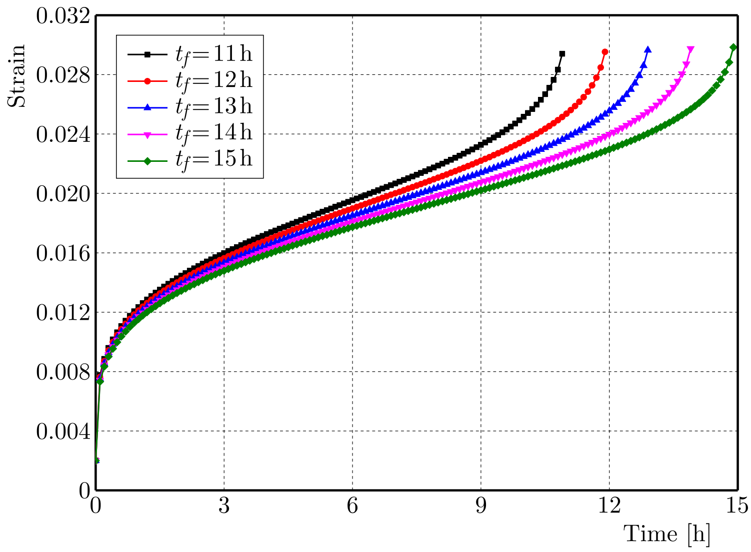

Fig. 11. Influence of t_f on the creep curve

Figure 11 shows that a change in t_f has significantly effect on the shape of the model creep curve. The smaller the value of t_f, the steeper the creep curve, and the faster the rate of increase in creep strain. In addition, t_f represents the time when the rock undergoes creep failure, therefore, the smaller t_f, the shorter the time for the rock to undergo creep failure.

5.4. The influence of n

Assuming $\sigma = 60\,\text{MPa}$, $\eta = 2.0 \cdot 10^{-12}\,\text{GPah}$, $E = 30\,\text{GPa}$, $t_f = 15\,\text{h}$, according to Eq. (2.5), the unsteady creep curves of rocks corresponding to different model orders n were obtained, as shown in Fig. 12.

As shown in Fig. 12, n has a significant influence on the shape of the creep curve of the model. As n increases, the creep strain simultaneously increases nonlinearly; that is, according to the order from bottom to top, the creep curve becomes increasingly sparse. Simultaneously, as the creep rate at the same time increased, the characteristics of accelerated creep became increasingly obvious, and the starting point of accelerated creep appeared earlier.

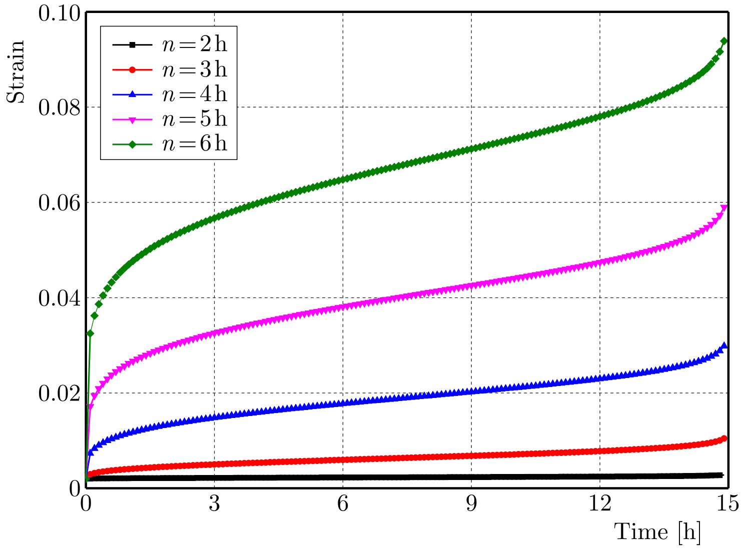

Fig. 12. Influence of n on the creep curve

6. Conclusions

Based on the antisymmetric relationship between the surface dynamic subsidence curve of coal mining and the unsteady creep curve of rocks, a rock unsteady creep model with four model parameters was established from the perspective of phenomenology using analogical reasoning. A simple and feasible method for determining the model parameters is provided based on the characteristics of the rock creep curve.

The rationality and accuracy of the four-parameter unsteady creep model were verified based on the compression creep data of four different rocks at different stress levels. The model not only describes the instantaneous strain stage, attenuation creep stage, and constant velocity creep stage of rocks at different stress levels, but also reflects the accelerated creep stage with particularly obvious nonlinear characteristics.

The unsteady creep strain of the rocks increases with an increases in the viscosity coefficient and model order. Under the same increment in the viscosity coefficient, the creep strain increment at the same time gradually decreases, whereas under the same increment in the model order, the creep strain increment at the same time gradually increases.

Acknowledgements

The authors would like to thank the editors and anonymous referees for detailed and valuable suggestions that helped to improve the original manuscript to its present form.

The research described in this paper was financially supported by Natural Science Research Project in the Universities of Anhui Province (No.KJ2021A1056).

References

1. Cao W.G., Chen K., Tan X., Chen T., 2020, A novel damage-based creep model considering the complete creep process and multiple stress levels, *Computers and Geotechnics*, **124**, 103599

2. Discenza M.E., Martino S., Bretschneider A., Mugnozza G.S., 2020, Influence of joints on creep processes involving rock masses: results from physical-analogue laboratory tests, *International Journal of Rock Mechanics and Mining Sciences*, **128**, 104261

3. Hejmanowski R., 2015, Modeling of time dependent subsidence for coal and ore deposits, *International Journal of Coal Science and Technology*, **2**, 287-292
4. Jin J.C., Yang F.W., Jing L.H., She C.X., Song Z.Y., 2024, New accelerated rock creep model considering nonstationary viscosity coefficient, *International Journal of Non-Linear Mechanics*, **159**, 104628
5. Kachanov M., 1992, Effective elastic properties of cracked solids: critical review of basic concepts, *Applied Mechanics Reviews*, **45**, 8, 304-335
6. Liu X.L., Li D.J., Han C., 2021, Nonlinear damage creep model based on fractional theory for rock materials, *Mechanics of Time-Dependent Materials*, **25**, 341-352
7. Song Y., Fan B., Li Y., Wang H., 2023, Research on creep-fatigue model of anchored jointed rock mass, *Journal of Theoretical and Applied Mechanics*, **61**, 1, 163-173
8. Song Y., Li Y.Q., 2022, Study on the shear creep characteristics of anchored jointed rock masses under creep fatigue loading, *Journal of Theoretical and Applied Mechanics*, **60**, 4, 625-635
9. Sterpi D., Gioda G., 2009, Visco-plastic behaviour around advancing tunnels in squeezing rock, *Rock Mechanics and Rock Engineering*, **42**, 319-339
10. Taheri S.R., Pak A., Shad S., Mehrgini B., Razifar M., 2020, Investigation of rock salt layer creep and its effects on casing collapse, *International Journal of Mining Science and Technology*, **30**, 3, 357-365
11. Wang J.B., Liu X.R., Song Z.P., *et al.*, 2018, A whole process creeping model of salt rock under uniaxial compression based on inverse S function (in Chinese), *Chinese Journal of Rock Mechanics and Engineering*, **37**, 11, 2446-2459
12. Wei F., Chen J., Zou Q.L., 2019, A nonlinear creep damage model for salt rock, *International Journal of Damage Mechanics*, **28**, 5, 758-771
13. Yan B.Q., Guo Q.F., Ren F.H., Cai M.F., 2020, Modified Nishihara model and experimental verification of deep rock mass under the water-rock interaction, *International Journal of Rock Mechanics and Mining Sciences*, **128**, 104250
14. Yang S.Q., Xu P., Ranjith P.G., 2015, Damage model of coal under creep and triaxial compression, *International Journal of Rock Mechanics and Mining Sciences*, **80**, 337-345
15. Yang W.D., Zhang Q.Y., Li S.C., Wang S., 2014, Time-dependent behavior of diabase and a nonlinear creep model, *Rock Mechanics and Rock Engineering*, **47**, 4, 1211-1224
16. Zhang K., Zhou H., Shao J.F., 2013, An experimental investigation and an elastoplastic constitutive model for a porous rock, *Rock Mechanics and Rock Engineering*, **46**, 6, 1499-1511
17. Zhang L.L., Cheng H., Yao Z.S., Wang X., 2020, Application of the improved Knothe time function model in the prediction of ground mining subsidence: A case study from Heze city, Shandong Province, China, *Applied Sciences*, **10**, 3147
18. Zhang L.L., Wang X.J., 2020, Viscoelastic-plastic damage creep model for rock (in Chinese), *Chinese Journal of Geotechnical Engineering*, **42**, 6, 1085-1092
19. Zhang Z.L., Xu W.Y., Wang W., 2011, Study of triaxial creep tests and its nonlinear visco--elastoplastic creep model of rock from compressive zone of dam foundation in Xiangjiaba hydropower station (in Chinese), *Chinese Journal of Rock Mechanics and Engineering*, **30**, 1, 132-140
20. Zhao Y.L., Liu Q., Tang L.M., Xie S.L., 2019, The double Burgers model of fractured rock masses considering creep fracture damage, *Journal of Vibroengineering*, **21**, 4, 974-987
21. Zhao Y., Yan H., Wu P., Zhou D., 2020, Linear correction method for improved atmospheric vertical profile retrieval based on ground-based microwave radiometer, *Atmospheric Research*, **232**, 104678
22. Zhong S.Y., Ma M.J., 1987, An approach to creep failure regularity of weak rock (in Chinese), *Journal of Central South University*, **18**, 5, 495-500

23. Zhou H.W., Wang C.P., Han B.B., Duan Z.Q., 2011, A creep constitutive model for salt rock based on fractional derivatives, *International Journal of Rock Mechanics and Mining Sciences*, **48**, 116-121

24. Zivaljevic S., Tomanovic Z., 2022, Loading history effect on time-dependent deformations after unloading – reversible creep of soft rock (marl), *Mechanics of Time-Dependent Materials*, **26**, 499-530

Manuscript received October 25, 2023; accepted for print February 8, 2024